Numerical modelling the influence of water content on the mechanical behaviour of concrete under high confining pressures

Yun Jia, Xiaolong Zhao, Hanbing Bian, Wei Wang, Jian-Fu Shao

▶ **To cite this version:**

Yun Jia, Xiaolong Zhao, Hanbing Bian, Wei Wang, Jian-Fu Shao. Numerical modelling the influence of water content on the mechanical behaviour of concrete under high confining pressures. Mechanics Research Communications, 2022, 119, pp.103819. 10.1016/j.mechrescom.2021.103819 . hal-04128284

HAL Id: hal-04128284

https://univ-artois.hal.science/hal-04128284

Submitted on 15 Feb 2024

HAL is a multi-disciplinary open access archive for the deposit and dissemination of scientific research documents, whether they are published or not. The documents may come from teaching and research institutions in France or abroad, or from public or private research centers.

L'archive ouverte pluridisciplinaire **HAL**, est destinée au dépôt et à la diffusion de documents scientifiques de niveau recherche, publiés ou non, émanant des établissements d'enseignement et de recherche français ou étrangers, des laboratoires publics ou privés.

Numerical modelling the influence of water content on the mechanical behaviour of concrete under high confining pressures

Yun Jia[a,b,*], Xiaolong Zhao[a,b], Hanbing Bian[c,**], Wei Wang[a], Jian-Fu Shao[a,b]

[a] *College of Civil and Transportation Engineering, Hohai University, Nanjing 210098, China*
[b] *Univ. Lille, CNRS, Centrale Lille, UMR 9013 - LaMcube - Laboratoire de Mécanique, Multiphysique, Multi-échelle, F-59000 Lille, France*
[c] *Univ. Lille, -LGCgE- Laboratoire de génie civil et géo-environnement, F-59000 Lille, France*

Abstract

The present paper focuses on the hydro-mechanical behaviour of concrete under high confining pressures. By using the poromechanics approach, an elastoplastic model is adopted to describe the mechanical behaviour of concrete under different saturation conditions and high confining pressures. A hydrostatic compression test with the measurement of interstitial pore pressure is firstly used to identify the model's parameter. After that, three quasi-oedometric tests with different water contents are simulated. The obtained numerical results exhibit that the mechanical behaviour of concrete is strongly coupled with its hydraulic responses. For instance: the saturation kinetics is accelerated by the plastic deformation related to pore collapse and volumetric compaction. The numerical predictions and discussions can help engineers to enhance their understandings on the influence of interstitial pore pressure on the vulnerability of concrete structures subjected to near-field detonations or impacts.

Keywords: Water saturation, Mechanical behaviour, Elastoplasticity, Pore collapse, Concrete, High confining pressure

1. Introduction

Massive concrete elements are widely used in civil and defence engineering applications, such as hydraulic dams and nuclear power plants. Due to the relatively low permeability of concrete, a heterogeneous distribution of free water content is generally observed in concrete structures: a quasi-saturated core combined with a fast drying surface. Numerous researches exhibit that free water content has an important impact on the mechanical behaviour of concrete [1–4]. During the lifetime of these concrete structures, they may be subjected to some accidental or extreme loadings, such as ballistic impact, earthquake, vehicle shocking or explosion. For instance, under the penetration of a rigid projectile with the velocity of 315 m/s [5], high triaxial stress states with a mean stress level up to 1 GPa are observed in concrete. In order to evaluate the vulnerability of concrete infrastructure subjected to near-field detonations or impacts, it is necessary to understand the influence of free water content on the mechanical behaviour of concrete under high confining pressures.

In view of this, different triaxial compression tests [6–10] have been performed to study the mechanical behaviour of concrete under a wide range of confining pressures and water contents. One observes that compressive/tensile strength of concrete decreases with increasing water content while volumetric stiffness of concrete increases with water content. These observations are due to the presence of pore water in concrete. However, due to the difficulties in the measurement of pore water pressure, few experimental works can be found in the literature. Recently, Accary et al. [11, 12] have performed a series of hydrostatic compression tests under different confining pressures (even up to 600 MPa). With the confining pressure of 500 MPa, a pore pressure of order 400 MPa is observed in saturated concrete. Meanwhile, one observes that the volumetric stiffness of concrete increases obviously with increasing pore water pressure. These experimental observations exhibit that the mechanical behaviour of concrete is strongly coupled with its hydraulic responses.

Numerical simulations have also been performed to study the influence of free water content on the mechanical behaviour of concrete under a wide range of confining pressures [13–19]. On one hand, some micromechanics-based simulations [13, 14] were realized to study the response of concrete under high confining pressures. Although the physical mechanisms and the influence of concrete aggregate structure are taken into account in these numerical simulations, their applications are limited on small sample scale as significant computational efforts are required for the engineering applications. On the other hand, for ease of use, some macroscopic studies have been realized on the basis of recent experimental studies. Zhou et al. [15] have used an elastoplastic damage to analyse the mechanical behavior of saturated concrete under a wide range of confining pressure. Afterwards, the influence of water content was taken into account by Yang et al. [16]. In 2018, Bian et al. [18] have used a modified Young's model to study the penetration of a rigid projectile into a concrete target. The penetration performance of saturated concrete was satisfactorily captured by the numerical simulations and the penetration responses of dry concrete were also predicted. Recently, by adopting the pore water pres-

*Corresponding authors: Yun.jia@polytech-lille.fr
**Corresponding authors: Hanbing.bian@polytech-lille.fr

sure as a function of volumetric strain, Huang et al. [19] have shown that the pore pressure played an important role in the ballistic penetration of concrete targets. Although the influence of free water content on the mechanical behaviour of concrete was considered, hydraulic responses (variation of fluid pressure with mass change and/or skeleton deformation) have not been analysed in these studies.

The present work aims to analyse the coupled hydromechanical behaviour of concrete under high confining pressures, with a special attention on the hydraulic responses of concrete. Concrete is represented by three-phase porous media: a solid matrix, pore water and gas mixture. By using the poromechanics approach, the recent proposed constitutive model [18] is adopted to capture the full coupling between mechanical and hydraulic behaviour of saturated/unsaturated concretes. The adopted numerical method and constitutive model is validated by simulating three quasi-oedometric compression tests with the variations of interstitial water pressure. Finally, the hydraulic responses of concrete are analysed and discussed to illustrate the relationship between pore water pressure and porosity of concrete.

2. Proposed elastoplastic model

The studied concrete is a standard concrete mixture, called R30A7 concrete, with a 28-days compressive strength of 30 MPa. Its composition is given in Vu [7]. As indicated in the experimental results, the mechanical behaviour of concrete is strongly influenced by the presence of pore water. Therefore, elastic response, failure strength as well as plastic behaviour are affected by pore water pressure. With the assumption of small evolutions and isothermal conditions, the total strain increment tensor $d\underline{\underline{\varepsilon}}$ is decomposed into an elastic part $d\underline{\underline{\varepsilon}}^e$ and a plastic one $d\underline{\underline{\varepsilon}}^p$:

$$d\underline{\underline{\varepsilon}} = d\underline{\underline{\varepsilon}}^e + d\underline{\underline{\varepsilon}}^p \tag{1}$$

2.1. Non-linear poroelastic behaviour

Concrete is assumed as an isotropic porous media partially saturated by a water phase (index w) and a gas mixture (index g). As the variation of gas pressure in the laboratory tests is extremely small with respected to that of liquid pressure, the variation of gas pressure is neglected in the present study $dp_{gz} = 0$. Considering the porous material subjected to macroscopic stress $d\underline{\underline{\sigma}}$ and liquid pressure dp_w, the poroelastic constitutive equations of unsaturated porous media can be written as follows [20, 21]:

$$\begin{cases} d\underline{\underline{\sigma}} = (K_b - \frac{2}{3}G)d\varepsilon_v^e\underline{\underline{\delta}} + 2Gd\varepsilon_{ij}^e - bS_w dp_w\underline{\underline{\delta}} \\ \frac{dm_w}{\rho_w} = N_{ww}dp_w + bS_w d\varepsilon_v^e \end{cases} \tag{2}$$

In these equations, K_b and G are respectively the drained bulk modulus and shear modulus of porous medium. ε_v^e represents elastic volumetric strain. S_w denotes water saturation degree. $\underline{\underline{\delta}}$ denotes the second-order unit tensor. The parameter b is the Biot's coefficient of porous medium, and $b = 0.6$ for studied concrete. The Biot's modulus N_{ww} can be identified as follows:

$$N_{ww} = \phi\frac{\partial S_w}{\partial p_w} + \frac{\phi S_w}{K_w} + NS_w^2, N = \frac{(1-b)(b-\phi)}{K_b} = \frac{(b-\phi)}{K_s} \tag{3}$$

In these relations, ϕ is the porosity, K_s denotes the bulk modulus of solid matrix. K_w represents the compressibility modulus of liquid water and one takes $K_w = 2000GPa$. With the assumption that water saturation depends only on pore water pressure p_w, p_w is related to S_w by the water retention curve:

$$S_w = [1.0 + (-p_w/a_w)^{b_w}]^{-(1-\frac{1}{b_w})}, a_w = 2.0E6, b_w = 1.54 \tag{4}$$

Under undrained condition ($dm_w = 0$), the evolution of pore water pressure can be obtained by using the Eq. (2):

$$dp_w = bS_w d\varepsilon_v^e / N_{ww} \tag{5}$$

2.2. Plasticity characterization

Based on the experimental investigation [6, 7], an elastoplastic damage model is required to study the mechanical behaviour of concrete under a wide range of confining pressures. Under low and moderate confining pressures, the plastic shearing mechanism leads to the failure of concrete by the formation of shear band and crack coalescence. When the applied stress attains a limit, the pore collapse process dominates the evolution of plastic deformation and material failure related to the shear bands/crack growth is relatively negligible. As the emphasize of the present study is put on the influence of free water content on the mechanical behaviour of concrete under high confining pressures, the damage is neglected and only two plastic deformations proposed by Bian et al. [18] are adopted in the present work.

Since two plastic mechanisms are observed in the studied concrete under triaxial compression conditions, the plastic part $d\underline{\underline{\varepsilon}}^p$ is divided into a shear plastic part $d\underline{\underline{\varepsilon}}^{ps}$ and a plastic pore collapse part $d\underline{\underline{\varepsilon}}^{pc}$:

$$d\underline{\underline{\varepsilon}}^p = d\underline{\underline{\varepsilon}}^{ps} + d\underline{\underline{\varepsilon}}^{pc} \tag{6}$$

In the literature, different kinds of approaches have been proposed for modelling poro-mechanical behaviour of saturated and unsaturated geomaterials. Among these approaches, two basic concepts have been widely used: the generalized effective stress approach and the so-called Barcelona's approach. As the Barcelona concept is fully based on the experimental investigation, this approach is adopted in the present work for the poro-plastic description of concrete. The plastic functions are expressed as functions of net stress $\underline{\underline{\sigma}}' = \underline{\underline{\sigma}} - p_{gz}\underline{\underline{\delta}}$ and water saturation degree S_w. In saturated case, gas pressure is replaced by water pressure , the net stress is then rewritten as $\underline{\underline{\sigma}}' = \underline{\underline{\sigma}} + bp_w\underline{\underline{\delta}}$.

2.2.1. Plastic shear characterization

Based on the experimental data obtained under various loading paths, a curved yield surface is necessary to describe its strong pressure dependence. Inspired by the constitutive model

proposed by Bian et al. [18], the following yield function is used:

$$F_s(\underline{\underline{\sigma}}', \gamma^{ps}, S_w) = q + \alpha_s(p - c_3)\frac{c_1}{(1 - c_2(S_w)\frac{p}{p_r})} = 0 \quad (7)$$

p is the mean stress and q denotes the deviatoric stress. p_r is a unit pressure, $p_r = 1$ MPa. The parameter c_1 is an equivalent friction coefficient. c_3 denotes the cohesion coefficient of material. c_2 defines the nonlinearity of yield surface. By using the peak stress obtained in triaxial compression tests, the values of parameters c_1, c_2, c_3 can be determined from the best fitting of the failure surface in the $p - q$ plan. As the experimental investigation exhibits that the curvature of deviatoric yield surface is dependent on S_w, the parameter c_2 is expressed as following:

$$c_2(S_w) = c_{2s} - (c_{2s} - c_{2d})e^{[-\xi_{c_2}S_w/(1-S_w)]} \quad (8)$$

The parameters ξ_{c_2} controls the evolution of c_2 with S_w. c_{2s}, c_{2d} are respectively the values of c_2 in fully saturated and dry concretes.

The plastic hardening parameter α_s is a function of generalized plastic distortion γ^{ps}:

$$\alpha_s = 1.0 - (1.0 - \alpha_s^0)e^{(-\zeta\gamma^{ps})}, \gamma^{ps} = \int \sqrt{\frac{2}{3}d\underline{\underline{e}}^{ps}d\underline{\underline{e}}^{ps}}/\chi_p \quad (9)$$

α_s^0 represents the initial value of α_s and can be determined by using the initial yield surface in the $p - q$ plan. The parameter ζ controls the kinetic of plastic hardening and can be identified from the $\alpha_s - \gamma^{ps}$ curve. The function χ_p is introduced to describe the strong pressure sensitivity of plastic hardening.

In order to describe the plastic volumetric transition from contraction to dilatancy, a non-associated plastic flow rule is used:

$$Q_s(\underline{\underline{\sigma}}', \gamma^{ps}, S_w) = q + \mu_s I ln(I/I_0) = 0, I = p - c_3 \quad (10)$$

The parameter I_0 defines the intersection of the plastic potential surface with the p axis. The parameter μ_s defines the slope of the volumetric transition boundary. By identifying the stress point where the volumetric strain rate is close to zero on stress–strain curves, the parameter μ_s can be obtained.

For the loading history where only the plastic shear mechanism is developed, the plastic flow rule is written as:

$$d\underline{\underline{\varepsilon}}^{ps} = d\lambda_s\frac{\partial Q_s}{\partial\underline{\underline{\sigma}}'}, \frac{\partial Q_s}{\partial\underline{\underline{\sigma}}'} = \frac{3}{2}\frac{\underline{\underline{s}}}{q} + \frac{1}{3}\mu_s[1 + (\frac{I}{I_0})]\underline{\underline{\delta}} \quad (11)$$

The plastic multiplier $d\lambda_s$ can be determined by the plastic consistency condition:

$$d\lambda_s = \frac{\frac{\partial F_s}{\partial\underline{\underline{\sigma}}'} : d\underline{\underline{\sigma}}' + \frac{\partial F_s}{\partial S_w}\frac{\partial S_w}{\partial p_w}dp_w}{\frac{\partial F_s}{\partial\underline{\underline{\sigma}}'} : \underline{\underline{\underline{\underline{C}}}} : \frac{\partial Q_s}{\partial\underline{\underline{\sigma}}'} - \frac{\partial F_s}{\partial\alpha_s}\frac{\partial\alpha_s}{\partial\gamma^{ps}}\sqrt{\frac{2}{3}(\underline{\underline{\underline{\underline{K}}}} : \frac{\partial Q_s}{\partial\underline{\underline{\sigma}}'}) : (\underline{\underline{\underline{\underline{K}}}} : \frac{\partial Q_s}{\partial\underline{\underline{\sigma}}'})}} \quad (12)$$

2.2.2. Plastic pore collapse characterization

Inspired by the plastic model proposed by Bian et al. [18], the following plastic yield function is used to describe the pore collapse mechanism observed under high confining pressures :

$$F_c(\underline{\underline{\sigma}}', \overline{\sigma}, \phi, S_w) = \frac{q^2}{\overline{\sigma}^2} + 2\phi\cosh(\frac{3p}{\overline{\sigma}}) - 1 - \phi^2 = 0 \quad (13)$$

The coefficient $\overline{\sigma}$ represents the plastic yield stress of solid matrix for the plastic pore collapse mechanism. Based on the experimental investigation of hydrostatic compression tests, a plastic isotropic hardening law is proposed:

$$\overline{\sigma} = \overline{\sigma}_0[1 + a(\varepsilon_M^{pc})^n e^{\eta\varepsilon_M^{pc}}], \varepsilon_M^{pc} = tr(\underline{\underline{\varepsilon}}^{pc}) \quad (14)$$

$\overline{\sigma}_0$ denotes the initial yield stress of solid matrix. a, n and η are three hardening parameters. These four parameters $(\overline{\sigma}_0, a, n, \eta)$ could be identified directly from a hydrostatic compression test. The parameter $\overline{\sigma}_0$ can be determined from the transition point from linear to non-linear part of the confining pressure P_c- volumetric strain ε_v curve. a, n, η can be determined by the best fitting of the P_c-$\varepsilon_v$curve. As the experimental observation exhibits that the kinetics of plastic pore collapse process is affected by water content, the parameter η, controlling the hardening kinetics of plastic pore collapse, is expressed as a function of S_w. For the reason of simplicity, an exponential function as that of the parameter c_2 is proposed for η:

$$\eta(S_w) = \eta_s - (\eta_s - \eta_d)e^{[-\xi_\eta S_w/(1-S_w)]} \quad (15)$$

The function $\eta(S_w)$ varies from the asymptotic value for saturated concrete η_s to the asymptotic value for dry concrete η_d. The parameter ξ_η controls the evolution of parameter η with S_w.

By assuming that the plastic compressibility of solid phase may be neglected, the porosity change, mainly due to the plastic pore collapse mechanism, is expressed as following [18]:

$$d\phi = \beta\phi(1 - \phi)tr(d\underline{\underline{\varepsilon}}^{pc}) \quad (16)$$

The parameter β controls the evolution of porosity.

As the plastic pore collapse mechanism focuses on the volumetric compaction observed under high confinement, the plastic potential is written as following:

$$Q_c(\underline{\underline{\sigma}}', \overline{\sigma}, \phi) = \frac{q^2}{\overline{\sigma}^2} + 2\phi\cosh(\frac{3p}{2\overline{\sigma}}) \quad (17)$$

For the loading history where only the plastic pore collapse mechanism is developed, the plastic flow is written by:

$$d\underline{\underline{\varepsilon}}^{pc} = d\lambda_c\frac{\partial Q_c}{\partial\underline{\underline{\sigma}}'}, \frac{\partial Q_c}{\partial\underline{\underline{\sigma}}'} = \frac{3\underline{\underline{s}}'}{\overline{\sigma}^2} + \frac{q_2\phi}{\overline{\sigma}}\sinh(\frac{3p}{2\overline{\sigma}})\underline{\underline{\delta}} \quad (18)$$

The plastic multiplier $d\lambda_c$ can be determined by the plastic consistency condition, as:

$$d\lambda_c = \frac{\frac{\partial F_c}{\partial\underline{\underline{\sigma}}'} : d\underline{\underline{\sigma}}' + \frac{\partial F_c}{\partial S_w}\frac{\partial S_w}{\partial p_w}dp_w}{\frac{\partial F_c}{\partial\underline{\underline{\sigma}}'} : \underline{\underline{\underline{\underline{C}}}}(\omega) : \frac{\partial Q_c}{\partial\underline{\underline{\sigma}}'} - \frac{\partial F_c}{\partial\overline{\sigma}}\frac{\partial\overline{\sigma}}{\partial\varepsilon_M^{pc}}tr(\frac{\partial Q_c}{\partial\underline{\underline{\sigma}}'}) - \frac{\partial F_c}{\partial\underline{\underline{\sigma}}'}\beta\phi(1 - \phi)tr(\frac{\partial Q_c}{\partial\underline{\underline{\sigma}}'})} \quad (19)$$

2.3. Coupling of two plastic mechanisms

Under general loading conditions, two plastic flows occur in the coupled process. Consequently, the plastic strain rates should be determined simultaneously. The plastic consistency condition is needed for the determination of plastic multipliers.

$$\begin{cases} dF_c = \frac{\partial F_c}{\partial \underline{\underline{\sigma'}}} d\underline{\underline{\sigma'}} + \frac{\partial F_c}{\partial \phi} d\phi + \frac{\partial F_c}{\partial \overline{\sigma}} \frac{\partial \overline{\sigma}}{\partial \underline{\underline{\varepsilon}}^{cp}} d\underline{\underline{\varepsilon}}^{cp} + \frac{\partial F_c}{\partial S_w} \frac{\partial S_w}{\partial p_w} dp_w = 0 \\ dF_s = \frac{\partial \overline{F}_s}{\partial \underline{\underline{\sigma'}}} d\underline{\underline{\sigma'}} + \frac{\partial F_s}{\partial \alpha_s} \frac{\partial \alpha_s}{\partial \gamma^{ps}} d\gamma^{ps} + \frac{\partial F_s}{\partial S_w} \frac{\partial S_w}{\partial p_w} dp_w = 0 \end{cases} \tag{20}$$

By introducing the state equations and the hardening law in the above equations, we obtain the system of equations to determine the plastic multipliers:

$$\begin{pmatrix} \frac{\partial F_c}{\partial \underline{\underline{\sigma'}}} : \underline{\underline{\underline{\underline{C}}}}(\omega) : \frac{\partial Q_c}{\partial \underline{\underline{\sigma'}}} - H_{cc} & \frac{\partial F_c}{\partial \underline{\underline{\sigma'}}} : \underline{\underline{\underline{\underline{C}}}}(\omega) : \frac{\partial Q_s}{\partial \underline{\underline{\sigma'}}} \\ \frac{\partial \overline{F}_s}{\partial \underline{\underline{\sigma'}}} : \underline{\underline{\underline{\underline{C}}}}(\omega) : \frac{\partial Q_c}{\partial \underline{\underline{\sigma'}}} & \frac{\partial F_s}{\partial \underline{\underline{\sigma'}}} : \underline{\underline{\underline{\underline{C}}}}(\omega) : \frac{\partial Q_s}{\partial \underline{\underline{\sigma'}}} - H_{ss} \end{pmatrix} \begin{pmatrix} d\lambda_c \\ d\lambda_s \end{pmatrix} = \begin{pmatrix} \frac{\partial F_c}{\partial \underline{\underline{\sigma'}}} : d\underline{\underline{\sigma'}} + \frac{\partial F_c}{\partial S_w} \frac{\partial S_w}{\partial p_w} dp_w \\ \frac{\partial \overline{F}_s}{\partial \underline{\underline{\sigma'}}} : d\underline{\underline{\sigma'}} + \frac{\partial F_s}{\partial S_w} \frac{\partial S_w}{\partial p_w} dp_w \end{pmatrix}$$

$$with \begin{cases} H_{cc} = \frac{\partial F_c}{\partial \phi} \beta \phi (1-\phi) tr(\frac{\partial Q_c}{\partial \underline{\underline{\sigma'}}}) + \frac{\partial F_c}{\partial \overline{\sigma}} \frac{\partial \overline{\sigma}}{\partial \varepsilon_M^{pc}} tr(\frac{\partial Q_c}{\partial \underline{\underline{\sigma'}}}) \\ H_{ss} = \frac{\partial F_s}{\partial \alpha_s} \frac{\partial \alpha_s}{\partial \gamma^{ps}} \sqrt{\frac{2}{3} (\underline{\underline{\underline{\underline{K}}}} : \frac{\partial Q_s}{\partial \underline{\underline{\sigma'}}}) : (\underline{\underline{\underline{\underline{K}}}} : \frac{\partial Q_s}{\partial \underline{\underline{\sigma'}}})} \end{cases} \tag{21}$$

The general formulation of the proposed model is capable of describing the hardening interaction between the two plastic mechanisms. The proposed model is then implemented in the finite element code THMPASA [21], which is devoted to numerical analysis of fully coupled hydromechanical boundary values problems in saturated and unsaturated conditions. The general algorithm flowchart for the *i* th loading step can be summarized in Fig. 1:

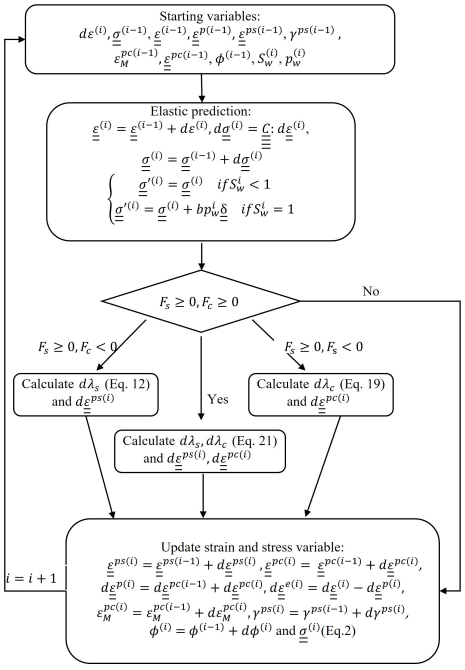

Figure 1: Flow chart for numerical implementation of the elastoplastic model at the *i*th step

2.4. Identification of model parameters

The detailed procedure for the identification of model's parameters is given by Bian et al. [18]. Their values are also given in Bian et al. [18], except the parameter β, which characterizes the porosity evolution in function of the applied stress. In the proposed constitutive model, the parameter β should be determined by drawing the evolution of porosity versus volumetric deformation. However, no corresponding experimental data is available in the literature. As the evolution of pore water pressure is essentially related to the porosity variation, β will be determined by drawing the evolution of water pressure versus volumetric deformation in a hydrostatic compression test.

Accary[11] have performed a series of hydrostatic compression tests. Under the confining pressure Pc=500MPa, one observes that the pore water pressure varies from 210 MPa to 425 MPa in saturated samples. By using the mean value of interstitial pore pressure obtained in the hydrostatic compression tests with $P_c = 500$ MPa, the value β is determined by the best fitting of the water pressure-volumetric strain curve and we obtain $\beta = 20$.

3. Numerical simulation of the laboratory tests

The main purpose of the present work is to study the influence of free water content on the mechanical behaviour of concrete under high confining pressures, with a special attention on the hydraulic responses of concrete. A fully coupled method is employed for the numerical modelling of hydro-mechanical behaviour of saturated and unsaturated concretes. The hydrostatic compression test with $P_c = 500$ MPa [11] and three quasi-oedometric compression tests with different initial water contents [11, 22] are simulated by using the adopted numerical method and constitutive model. The numerical simulations have been carried out under axisymmetric condition. Both stress and strain are taken to be positive in compression.

3.1. Hydrostatic compression test

The numerical results of the hydrostatic compression test with Pc=500MPa are firstly studied. The evolutions of water pressure p_w and porosity ϕ are given in Fig. 2. Three phases are generally observed in two curves. At the beginning, when the hydrostatic pressure is less than the pore collapse yield stress $\overline{\sigma}$, the pore collapse mechanism is not activated and the ratio of the actual porosity ϕ to its initial value ϕ_0 (i.e. ϕ/ϕ_0) is unchanged. Meanwhile, water pressure increases linearly with volumetric compaction. When the confining pressure exceeds the pore collapse limit, pores change with a high incidence of deformation and lead to a rapid decline in porosity, accompanied with a rapid increase of water pressure. With the gradual increase of confinement, the pores are further compressed. When the pores are difficult to be compressed continually, a slow decline is observed in porosity. In the later stage of experiment, as the pores cannot be changed continually, porosity decreases slightly with a gentle curve. In general, a good agreement is obtained between the numerical simulations and experimental data, especially the evolution of interstitial pore pressure.

In Fig. 3, the relationship between confining pressure P_c and volumetric deformation ε_v is presented. Three stages are also distinguished. One elastic phase, represented by the linear line, is firstly observed. Afterwards, when P_c is greater than $\overline{\sigma}$, the pores are compressed and a rapid increase of interstitial pore pressure is observed. As a result, the P_c-ε_v curve becomes non-linear. With the increase of hydrostatic pressure, the pores are compressed and concrete becomes stiffer. Finally, a rapid increase of confining pressure is observed at the end of test. However, this final rapid increase of confining pressure is not well captured by the numerical simulation. This observation may be explained by the fact that a constant bulk modulus of water is used in the simulation. In practice, the bulk modulus of water is a function of applied stress under undrained conditions. Again, the experimental data is satisfactorily reproduced by the numerical simulation. As the hydrostatic compression test has been used to identify the model's parameters, the comparison represents only a verification of the consistency of determined parameters. Therefore, three quasi-oedometric compression tests realized by Piotrowska et al. [11, 22] are simulated to verify the performance of adopted numerical method and constitutive model.

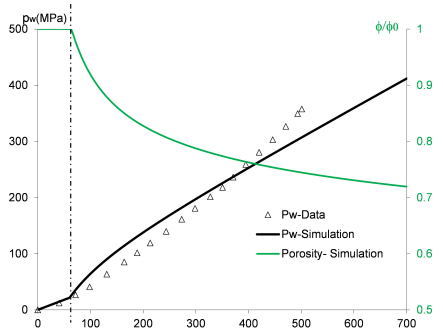

Figure 2: Evolution of ϕ/ϕ_0 and p_w in the hydrostatic compression test (Continuous line: numerical prediction; Cloud points: experimental data)

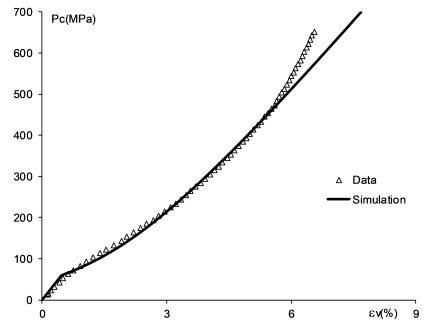

Figure 3: Simulation of P_c-ε_v curve of the hydrostatic compression test

3.2. *Quasi-oedometric compression tests*

In a static quasi-oedometric compression test, the specimen is tightly enclosed in a confinement vessel and compressed by an axial stress. As a result, the responses of concrete can be studied at a very high level of confining pressure. Three laboratory tests have been preformed by using the samples with three initial saturation degree S_w = 100%, 80% and 60%. In the numerical simulation, the horizontal displacements are fixed on the lateral boards of sample while the vertical displacement is blocked only on the bottom of sample. The external stress is applied on the upper board of the sample. Moreover, all the boards are impermeable.

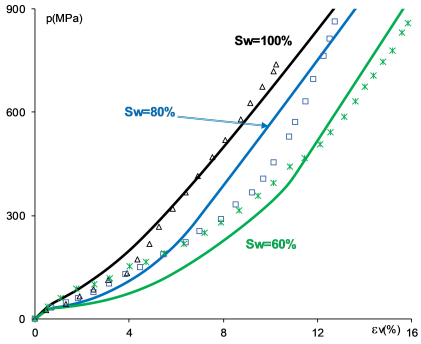

Figure 4: Simulation of mean pressure p-volumetric strain ε_v curves of three quasi-oedometric compression tests with S_w = 100%, 80% and 60%

The numerical results of three quasi-oedometric compression tests are presented in this section. The mean stress p-volumetric strain ε_v curves are firstly presented in Fig. 4. Three phases can be identified. One linear line, which represents the elastic phase, is firstly observed. Once the applied stress is greater than $\overline{\sigma}$, concrete samples exhibit important plastic deformation related to pore collapse and strong material compaction. When the pores cannot be compacted continually, a rapid increase of mean stress p is observed at the end of numerical simulation. By comparing three curves with different initial saturation degree S_w, one observes that the volumetric compressibility increases with increasing water saturation. The stiffest mean stress curve is obtained in the saturated case. According to the deviatoric stress q - mean stress$p$ curve, an increase of shear strength is observed when S_w decreases. The dependence of mechanical behaviour of concrete on the free water content is satisfactorily reproduced by the numerical simulations.

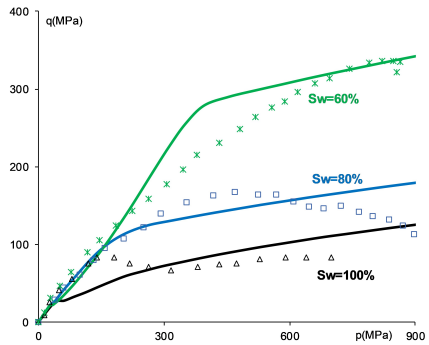

Figure 5: Simulation of the deviatoric stress q -mean stress p curves of three quasi-oedometric compression tests with S_w = 100%, 80% and 60%

The influence of water content on the mechanical behaviour of concrete can be explained by the following competition phenomena. When concrete is unsaturated, capillary pressure plays

a similar role as the confining pressure, certain microcracks can be re-closed and the interface between the aggregate and cement matrix is strengthened by a greater adhesion. Consequently, the resistance of concrete increases as the water saturation decreases. Meanwhile, the presence of free water may reduce the friction, created on the interfaces of reclosed microcracks. The increase of shear strength (Fig. 5) can be explained by the predominant confining pressure effect of capillary pressure. With the increase of applied stress, the volumetric compaction induced by pore collapse occurs and the unsaturated samples are progressively saturated. Therefore, due to the high compressibility of solid phase, the mean stress-volumetric strain curves become stiffer at the end of laboratory tests (Fig. 4). In general, a good concordance is obtained between the experimental data and numerical simulations.

3.3. Discussions

The principal results of three quasi-oedometric compression tests are compared and analysed in this section. The variation of interstitial pore pressure p_w and the evolution of saturation degree S_w are firstly analysed (Fig.6 and Fig.7).

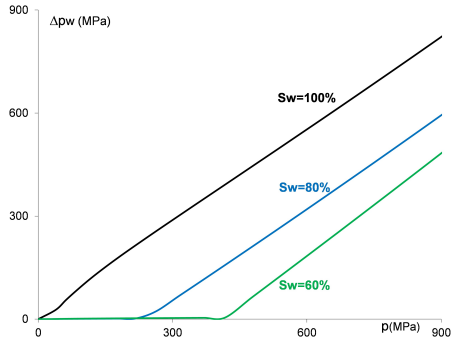

Figure 6: Variations of p_w in quasi-oedometric compression tests

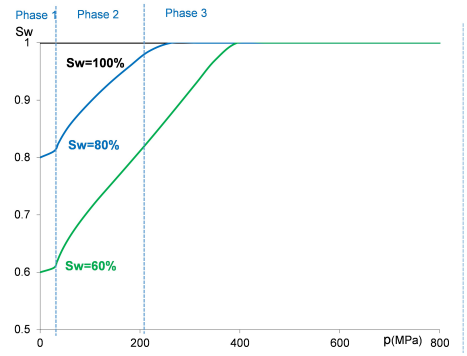

Figure 7: Evolution of S_w in quasi-oedometric compression tests

In the saturated case, as the pores are initially fulfilled with water, p_w increases immediately once the sample is compressed. Finally, a maximum water pressure of order 800 MPa are observed when the mean stress is equal to 900MPa (Figs. 6). On the other hand, in initially unsaturated cases ($S_w = 60, 80\%$), some of pores are filled with air, which can be compressed easily. Consequently, two samples are saturated gradually with increasing applied stress (Fig. 7). Once $\overline{\sigma}$ is attained, pore collapse occurs and volumetric compaction is then observed. As a result, two unsaturated samples are quickly saturated with pore closure (Fig. 7). Due to the increase of sample stiffness, the saturation process is decelerated. With respect to the sample $S_w = 80\%$, a slower resaturation process is observed in the sample $S_w = 60\%$ due to the presence of larger volume of air. Finally, when all the pores are filled with free water, the initially unsaturated samples ($S_w = 60\%$ and 80%) become saturated. A rapid increase of interstitial pore pressure is then observed in three samples (Figs. 6).

The evolutions of porosity are compared in Fig. 8. According to the ratio ϕ/ϕ_0, three phases are also observed: the ratio is unchanged before the applied stress is smaller than $\overline{\sigma}$; after that, it decreases strongly with increasing applied stress; at the last stage, ϕ/ϕ_0 tends to a constant value. By comparing three curves with different S_w, the smallest variation of porosity is observed in the initially saturated sample ($S_w = 100\%$). The variations of pore water pressure are also given on the logarithmic scale (Fig.9). Once two initially unsaturated samples ($S_w = 80\%, 60\%$) are fully saturated, the pore water pressure curves approach progressively to each other with the continual volumetric compaction.

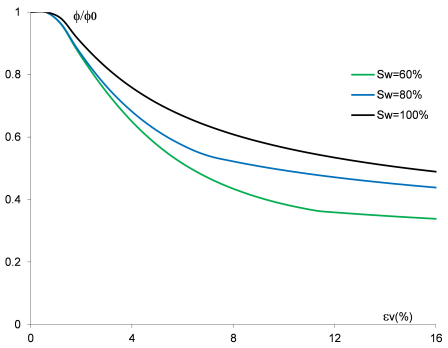

Figure 8: Variation of ϕ/ϕ_0 in quasi-oedometric compression tests

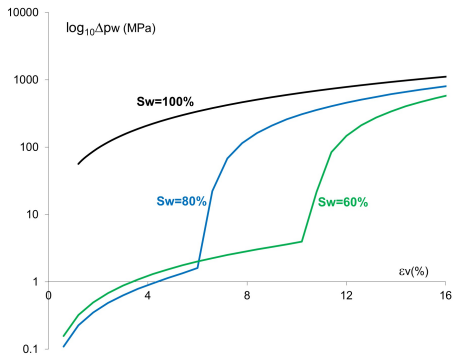

Figure 9: Variation of p_w in quasi-oedometric compression tests

Due to the low permeability of studied concrete, a total dry sample is extremely difficult to achieve experimentally without the destruction of its initial microstructure. In order to illus-

trate the influence of interstitial pore pressure on the response of saturated concrete, another calculation is realized by using the same parameters of initially saturated concrete without the consideration of interstitial pore pressure, called numerically dry case (i.e., $p_w = 0$). The numerical results of two cases are compared in Fig. 10. When the applied confining pressure exceeds the pore collapse yield stress, the influence of pore pressure is clearly identified: for a given level of mean stress, a more important decrease of deviatoric stress and porosity is observed in the numerically dry concrete ($p_w = 0$). This observation is related to the fact that the volume decrease of saturated concrete creates an increase of pore water pressure and then induces a decrease of effective stress applied on the solid skeleton. On the other hand, the applied stress is only carried by the solid skeleton in the case without water. Based on the previous results, we can conclude that the mechanical behaviour of concrete is strongly coupled with its hydraulic responses. For instance: the saturation process of concrete is accelerated by the plastic deformation related to pore collapse.

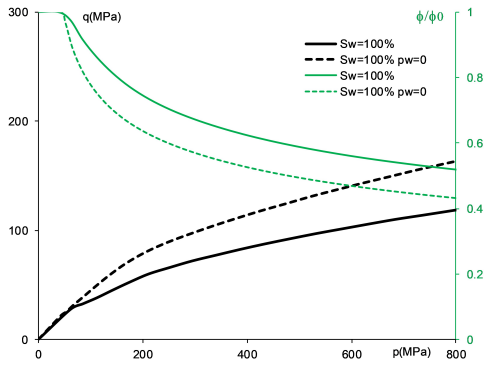

Figure 10: Evolutions of q and ϕ/ϕ_0 in the hydrostatic compression test

4. Conclusions

The fully coupled hydro-mechanical behaviour of concrete under high confining pressures is studied in the present study. The obtained results exhibit that interstitial pore pressure has an important impact on the confined responses of concrete: irreversible deformation, pore collapse and pressure dependence, etc... Generally, shear strength of concrete decreases with increasing water content while its volumetric stiffness increases with S_w. Moreover, a more important pore closing is observed in confined unsaturated concrete samples with respected to saturated one. The good concordance obtained between the experimental results and numerical simulations confirm that the adopted numerical method and constitutive model are capable of reproducing satisfactorily the interstitial pore pressure in confined saturated/unsaturated concrete under high confining pressures. In the near future, the proposed model will be used to study the penetration performance of concrete structures with the presence of pore water.

References

[1] S. Multon, F. Toutlemonde, Water distribution in concrete beams, Mater Struct 37 (6) (2004) 378–386.

[2] J. Zhang, H. Dongwei, S. Wei, Experimental study on the relationship between shrinkage and interior humidity of concrete at early age, Mag Concrete Res 62 (3) (2010) 191–199.

[3] S. E. Pihlajavaara, A review of some of the main results of a research on the ageing phenomena of concrete: Effect of moisture conditions on strength, shrinkage and creep of mature concrete, Cement Concrete Res 4 (5) (1974) 761–771.

[4] S. Popovics, Effect of curing method and final moisture condition on compressive strength of concrete, in: Journal Proceedings, Vol. 83, 1986, pp. 650–657.

[5] P. Forquin, A. Arias, R. Zaera, Role of porosity in controlling the mechanical and impact behaviours of cement-based materials, Int J Impact Eng 35 (3) (2008) 133–146.

[6] T. Gabet, Y. Malécot, L. Daudeville, Triaxial behaviour of concrete under high stresses: Influence of the loading path on compaction and limit states, Cement Concrete Res 38 (3) (2008) 403–412.

[7] X. H. Vu, Y. Malecot, L. Daudeville, E. Buzaud, Experimental analysis of concrete behavior under high confinement: Effect of the saturation ratio, Int J Solids Struct 46 (5) (2009) 1105–1120.

[8] X. H. Vu, L. Daudeville, Y. Malecot, Effect of coarse aggregate size and cement paste volume on concrete behavior under high triaxial compression loading, Constr Build Mater 25 (10) (2011) 3941–3949.

[9] C. Poinard, E. Piotrowska, Y. Malecot, L. Daudeville, E. N. Landis, Compression triaxial behavior of concrete: the role of the mesostructure by analysis of X-ray tomographic images, Eur J Environ Civ En 16 (sup1) (2012) s115–s136.

[10] Y. Malecot, L. Daudeville, F. Dupray, C. Poinard, E. Buzaud, Strength and damage of concrete under high triaxial loading, Eur J Environ Civ En 14 (6-7) (2010) 777–803.

[11] A. Accary, Experimental characterization of the interstitial pore pressure of wet concrete under high confining pressure, Ph.D. thesis, Université Grenoble Alpes (2018).

[12] A. Accary, L. Daudeville, Y. Malecot, Interstitial pore pressure in concrete under high confinement pressure: measurement and modelling, in: Proceedings of the 10th International Conference on Fracture Mechanics of Concrete and Concrete Structures FraMCoS-X, France, 2019.

[13] T. H. Le, L. Dormieux, L. Jeannin, N. Burlion, J.-F. Barthélémy, Nonlinear behavior of matrix-inclusion composites under high confining pressure: application to concrete and mortar, Comptes Rendus Mécanique 336 (8) (2008) 670–676.

[14] V. Tran, F. Donze, P. Marin, Discrete element model of concrete under high confining pressure, in: Proceeding of the 7th International Conference on Fracture Mechanics of Concrete and Concrete Structures, Vol. 1, 2010, pp. 481–486.

[15] H. Zhou, H. Bian, Y. Jia, J.-F. Shao, Elastoplastic damage modeling the mechanical behavior of rock-like materials considering confining pressure dependency, Mechanics Research Communications 53 (2013) 1–8.

[16] H. Yang, Y. Jia, J.-F. Shao, C. Pontiroli, Numerical analysis of concrete under a wide range of stress and with different saturation condition, Materials and Structures 48 (1) (2015) 295–306.

[17] P. Forquin, L. Sallier, C. Pontiroli, A numerical study on the influence of free water content on the ballistic performances of plain concrete targets, Mech Mater 89 (2015) 176–189.

[18] H. Bian, Y. Jia, C. Pontiroli, J.-F. Shao, Numerical modeling of the elastoplastic damage behavior of dry and saturated concrete targets subjected to rigid projectile penetration, Int J Numer Anal Methods Geomech 42 (2) (2018) 312–338.

[19] X. Huang, X. Kong, J. Hu, X. Zhang, Z. Zhang, Q. Fang, The influence of free water content on ballistic performances of concrete targets, Int J Impact Eng 139 (2020) 103530.

[20] O. Coussy, Poromechanics, John Wiley & Sons, 2004.

[21] Y. Jia, H. Bian, K. Su, D. Kondo, J.-F. Shao, Elastoplastic damage modeling of desaturation and resaturation in argillites, Int J Numer Anal Methods Geomech 34 (2) (2010) 187–220.

[22] E. Piotrowska, P. Forquin, Experimental characterization of the confined behaviour of concrete: influence of saturation ratio and strain-rate, Report, Université Grenoble Alpes, G3S laboratory (2013).